Advanced Planning and Intra-operative Validation for Robot-Assisted Keyhole Neurosurgery In ROBOCAST

Seyed-Ahmad Ahmadi, Tassilo Klein, Nassir Navab, Ran Roth, Reuben R Shamir, Leo Joskowicz, Elena DeMomi, Giancarlo Ferrigno, Luca Antiga, Roberto Israel Foroni

***Abstract*— ROBOCAST is a multi-national project comprising several institutes which aim at outlining and implementing a prototype system for advanced, robot-assisted keyhole neurosurgery. This paper reports mainly on software and sensor aspects of the system in the pre- and intra-operative stage. We describe a comprehensive workflow of planning steps provided to the surgeon in a wizard-like manner. As a novelty, we present a method for automatic trajectory planning based on a statistical and patient-specific risk atlas. Intra-operative monitoring of system uncertainty is proposed. Furthermore, the usage of 2D and 3D Freehand Ultrasound for intra-operative validation is motivated and theoretically outlined. After the first of three years project runtime, we present current work in progress and preliminary results on several patient studies concerning automatic path planning, trajectory localization errors as well as ultrasound imaging on one, six and three patients, respectively. The results underline the usefulness and significance of proposed methods, both within the scope of the ROBOCAST project as well as for conventional keyhole neurosurgery.**

I. INTRODUCTION

The project ROBOCAST aims at combining several existing and novel approaches from the communities of neurological and neurosurgical research, medical robotics, computer-assisted surgery and medical imaging into an overall system. Effectively, it should allow safer, more precise and more functional planning and execution of neurosurgical procedures through a keyhole. Within the project runtime of three years, the consortium of ROBOCAST is building and implementing a protoype and investigating the advantages and limits of such a highly integrated system within phantom and eventually cadaver studies. It will feature a combination of two robots, one for gross-positioning and one for fine-positioning together with actuators for a linear and – as a novelty – a flexible biomimetic probe for reaching of single and multiple targets in the brain.

S.-A. Ahmadi, T. Klein and N.Navab are with the Chair for Computer Aided Medical Procedures (CAMP), Institut für Informatik, Technische Universität München, GERMANY. [ahmadi, kleint, navab]@cs.tum.edu

R. Roth, R.R. Shamir and L. Joskowicz are with the School of Engineering and Computer Science, The Hebrew University of Jerusalem, ISRAEL. [ranroth, rubke, josko]@cs.huji.ac.il

E. DeMomi and G. Ferrigno are with the Bioengineering Department, Politecnico of Milan, ITALY. [elena.demomi, giancarlo.ferrigno]@polimi.it

L. Antiga is with the Medical Imaging Unit, Biomedical Engineering Department, Mario Negri Institute, Bergamo, ITALY. antiga@marionegri.it

R.I. Foroni is with the Department of Neurological and Visual Sciences, University of Verona, ITALY. roberto.foroni@univr.it

This work was supported by EU grant FP7-ICT-2007-215190.

In this paper, we report on several software aspects of the proposed system. Mainly, we present our progress of activities towards advanced pre-operative planning and intra-operative validation within the ROBOCAST project. After the first of three years runtime, the scope of activities were defined and first steps towards the realization of system features have been taken. Due to the complexity of the project and the extent of planned features, our work and also this paper focus mainly on implementation and integration of existing methods. Additionally, we present a novel approach for pre-operative planning based on a risk atlas and risk minimization for automatic path proposition to the surgeon. Overall, the scope of this paper is to introduce the planned and partially implemented ROBOCAST system and give a detailed overview of planned features. Although we are still at the beginning of the project and cannot present a thorough system evaluation or validation at this stage, we are showing preliminary results on different aspects of the presented approaches.

The rest of the paper is organized as follows. After a review of related literature, we give an in-depth description of the pre-operative planning workflow, which we provide to the surgeon in a wizard-like manner. Next, we present methods used for creation of a risk atlas and automatic proposition of low-risk trajectories during pre-operative planning. Furthermore, we describe the background for the calculation and visualization of uncertainty that the system is featuring pre- and intra-operatively. Subsequently, we describe the motivation and theory for usage of 3D Freehand Ultrasound within the ROBOCAST system.

In the following section on our current progress, we describe the outcome of a single-patient study on automatic path planning based on a simplified risk atlas featuring only blood vessels. Additionally, we present results from a study on localization error and uncertainty in six patients. In the last section, we present first results from transcranial ultrasound scans both in 2D and 3D on two patients who recently underwent DBS surgery. The results indicate the usability and relevance of ultrasound imaging as a validation tool in the ROBOCAST system.

II. RELATED WORK

In this paper, we report on four main software and sensor features of ROBOCAST, namely our workflow for advanced pre-operative planning, an advanced risk atlas for automated proposition of paths with lowest risk, the incorporation of uncertainty along the trajectory and the usage of 2D and

3D Freehand Ultrasound for intra-operative validation. We compare our work to a few selected pieces of literature for each of the four topics in this section.

Path planning in keyhole neurosurgery is a tedious task if done fully manually. The first step is to define a target point. Next, possible entry areas on the head outer surface are defined. For each entry point that is considered, the surgeon then has to carefully examine for each slide in the MRI, whether the trajectory is crossing critical anatomy such as blood vessels.

There are several groups that have proposed methods for automated trajectory computation. The relevance for automated path planning becomes clear in the work of Brunenberg et al. [11]. Their partnering neurosurgeons estimate a time gain of 30 minutes during pre-operative planning when using the authors' method for automated trajectory proposition, which effectively means that the planning time is halved. A segmentation of anatomy is performed in terms of blood vessels, ventricles and sulci of the cortex. An Euclidean distance map allows the calculation of paths with maximum distance to critical structures and thus minimal risk. Similar work as in [11] is presented in [15], [18] and [19]. In contrast to their work, we utilize a more extensive protocol of patient data acquisition in ROBOCAST including fMRI and DTI fibre imaging, which allows further incorporation of critical structures into a more extensive risk map than in above cited works.

As described in section III-A, we use a combination of patient-specific and statistical atlasses to provide our trajectory computation with advanced prior knowledge. D'Haese et al. propose the usage of an electrophysiological (EP) atlas for optimal placement of DBS electrodes in order to overcome the non-visibility of the target in the MRI, e.g. the sub-thalamic nucleus (STN) [16]. While they use their atlas mainly for finding the STN target, we use our risk atlas mainly for automatic computation of an entire trajectory, including entry point and target. A sophisticated atlas based on 3D histological information has been generated and presented in by Yelnik et al. [12]. As a prototype system for feasibility studies, ROBOCAST is going to investigate the usage of advanced atlasses for automated planning. We consider both cited works complementary to our approaches and hope that our work will encourage the merging of advanced data maps for improved neurosurgical planning in future.

In particular with respect to the tight spatial margins that are prevalent in neurosurgical planning [21], it becomes important to consider geometrical uncertainties along the planned trajectory. Simpson et al. [13] claim that it might be useful to visualize system uncertainty to the surgeon. They visualized the error in a patient-to-CT registration which effectively transformed a straight linear trajectory into an hourglass shape. The presentation of such uncertainty reduced the number of attempts in a simplified needle penetration task by approx. 40%. We extend this approach to intra-operative errors that stem from optical tracking uncertainty and visualize it to the surgeon as described in section III-D.

In order to validate the pre-operatively planned trajectory, we plan to incorporate 2D and 3D Freehand Ultrasound. The SonoWand system [14] is a commercially available system for 3D Freehand Ultrasound navigation of neurosurgical procedures under open craniotomy. In contrast to [14], we plan to investigate the usability of ultrasound in keyhole surgery using two minimally-invasive access ports – one transcranially and one through the burr-hole prior to opening of the dura mater. Transcranial ultrasound is particularly attractive due to its low requirements concerning sterility and it can be used for high-quality imaging of intracranial macro-vasculature [20]. This enables the surgeon to assess tissue shifts intra-operatively [14].

III. MATERIALS AND METHODS

A. Guided Pre-operative Planning of Keyhole Neurosurgery in ROBOCAST

The pre-operative planning phase has been organized into a multi-step wizard, where the surgeon is walked through a workflow of steps with well-defined functionality. The wizard and pre-operative planning visualization have been integrated within the Slicer 3D software. This workflow also serves as a comprehensive overview of system features incorporated in ROBOCAST. The wizard steps have been organized as follows:

1. Data loading: A group of steps where all available DICOM image series are parsed and loaded in the system. Series are either tagged as mandatory (3 Tesla T1 MRI, MRA) or optional (DWI, fMRI, CT, CTA).

2. Registration and segmentation: Based on the data loaded at the previous steps, the user submits a set of automated jobs to a high performance computing (HPC) cluster for the execution of: a) multimodal registration (all patient datasets and pre-computed DTI fiber bundles are registered on the 3 Tesla T1 MRI dataset, whose space is taken as a reference for all subsequent operations); b) atlas based segmentation, i.e. the T1 dataset of the SPL atlas [1] is registered on the 3 Tesla T1 MRI patient dataset using the *diffeomorphic demons* registration algorithm [2], and the labeling provided with the SPL atlas is employed to define anatomical areas on the patient's scan using a template matching segmentation strategy; c) skin surface segmentation: the head surface is automatically segmented from a 3 Tesla T1 MRI scan; d) fiducial segmentation: gadolinium markers are automatically identifed on the 3 Tesla T1 MRI scan and a model of the head-ring fixing the patient's head is placed within the reference scan space; e) vessels are segmented using a vessel enhancement approach [3], [4] followed by skeletonization of the segmented structures [5]. Jobs are executed in parallel using a shared-memory multi-threading approach with one job for each 8-processor node of a HPC cluster. Results are automatically loaded back on the pre-operative workstation upon completion of all jobs on the HPC cluster.

3. Verification: The user is allowed to review the results generated in the previous step, one task at a time, using advanced visualization. Scenes are automatically set-up by the system on the basis of the verification task. At the present time, in case the user judges a task to have been performed unsatisfactorily, we envision the following possibilities: a) making the user (or a specialized technician) access *advanced* parameter panes and resubmit a particular task on the HPC cluster; b) perform manual editing of the results (typically to correct anatomical area or vessel segmentation).

4. Lesion segmentation: The user manually delineates the lesion, with the possibility of switching between the available multimodal image datasets and performing fused visualization.

5. No-go area delineation: The user is required to manually delineate regions to be avoided by the trajectory either by specifying simple geometric entities (e.g. planes) or by directly classifying voxels (similarly to the lesion segmentation step).

6. Target selection: The user interactively specifies one target point in the case of a linear trajectory, or multiple target points in the case of a flexible probe and multi-target treatment.

7. Entry area selection: The user interactively selects an area on the skin surface to be considered as the candidate region for trajectory entry.

8. Trajectory computation: Based on a risk atlas, an automatic trajectory is computed as described in section III-B. A specified number of trajectories (three by default) are presented to the surgeon in order of increasing risk.

9. Trajectory verification: The user is given the possibility of reviewing the trajectories identified by the system as being associated to the least risk, and additionally of interactively moving the entry point in order to explore alternative trajectories. The system informs the user about the risk of the new trajectory resulting from the interactively defined entry point, in comparison to the automatically identified trajectories. During trajectory verification, the user is presented with an animated *probe's eye* view allowing the user to evaluate the path relative to the pre-operative imaging datasets.

10. Simulation: A High-Level Controller (HLC), which is present in the ROBOCAST system for execution of a pre-defined probe trajectory, features a simulation of the robot movements to ensure patient safety and avoid collision with objects in the OR. In step 10, this simulation is incorporated into the pre-operative planning workflow. The pre-segmented head outer surface, the entry point of several trajectories selected in step 9 and the target point are transferred to the HLC's simulator module. A registration of the patient images to the robot's dynamic reference frame (DRF) allows the trajectory information to be aligned with the robot coordinate system in a spatially correct manner. In an interactive 3D visualization of the robots with the patient and further objects in the OR, the surgeon can layout the surgery room pre-operatively until it is made sure that the robots can execute the planned trajectory. Upon entering the intra-operative phase, the robot-to-patient registration is achieved with a tracking camera and registration procedure integrated in the Prosurgics Pathfinder robot [23].

B. Automatic Trajectory Planning Based On A Risk Atlas

As a first step to test our approach we have created a risk volume computed from a head MRI that incorporates two major risk factors defined by the neurosurgeons: the blood vessels and user defined no-contraction zones where a surgical tool should not be placed because of clinical reasons. In clinical reasons we refer not only to risky structures that appear in the image and which can be segmented manually, but also to other structures or tissues that are not seen in the image and whose location is estimated by the neurosurgeons via nearby anatomical landmarks.

The risk volume is computed as follows. At first, the blood vessels are manually segmented and no-contraction zones are defined manually using the ITK-SNAP software package [6]. Then, a distance map is computed on the unified segmented volumes using the method suggested by Danielson P. E. [7] and as implemented in the Insight Segmentation and Registration Toolkit (ITK)(Kitware, USA). The risk volume is then computed as the inverse of the distance map such that a voxel that is further from the segmented zones is assigned with a lower risk value.

Subsequently, the optimal path is computed automatically as follows. At first, the neurosurgeon selects a preferred target on the MRI image. Then, the outer surface of the head is reconstructed as described in [8] and evenly sampled with 40,000 points. Each point is considered as a candidate entry point and with the target it defines a candidate path. Path's risk is computed as the maximal risk value along the path in the previously computed risk volume. In addition, the geometrical risk values are computed and presented to the neurosurgeon.

Currently, we are building a richer risk atlas that is more complex both in the number of considered risk factors and in the way of risk computation. Risk information will on the one hand be drawn from a multi-patient *statistical atlas*, namely the SPL atlas [1], which can be registered on the patient data using MRI images. On the other hand, risk information is drawn from *several patient-specific maps*, such as the already mentioned vessel distance map, functional area maps defined by the neurosurgeon from fMRI data and also neurological fiber information which is obtained from DTI imaging. Moreover, in the next version of the atlas the different risk factors are weighted such that areas related with higher risk to the patient will be assigned larger weights. We register this combined atlas data with the specific patient image and use it to compute the optimal, i.e. safest path.

C. Localization Error Measures

We define four clinically relevant localization error measures for keyhole neurosurgery: 1) Target Registration Error (TRE) - the distance between the planned and actual surgical tool tip location; 2) Entry Registration Error (ERE) - the distance between the planned and actual surgical tool entry point; 3) Angular Registration Error (ARE) - the angle between the planned and actual surgical tool trajectory, and; 4) Shift Registration Error (SRE) - the distance between the closest points on the planned and actual surgical tool trajectories. In general, the TRE cannot be derived from the other measures and the measures might have unknown dependencies. The implanted catheter was identified accurately (smaller than 0.3mm) on the postoperative image by repetitive selections of the entry, target, and trajectory points at different times. In three of the six cases, the entry point could not be identified accurately (larger than 0.5mm), so its location was discarded. The 3D localization errors were then computed from the 2D measurements obtained on orthogonal planes.

D. Uncertainty Propagation Intra-operatively

Navigation systems for intra-operative guidance require pose estimation of both patient and instruments. As employed in most commerically available systems, optical tracking is used for validation of robot and probe positions in the ROBOCAST system. As a first step for intra-operative uncertainty calculation, we consider the system uncertainty that is contributed from inaccuracies in optical tracking of objects. In current surgical navigation systems, the surgeon might be relying on false information if accuracy of optical localization falls beneath a certain threshold. A calculation and visualizaton of system inaccuracy should give the surgeon online feedback about the reliability of displayed information. A typical tracking system consists of a n-occular synchronized camera system, using linear, CCD or matrix cameras. In order to determine the pose of an instrument or patient, a marker body has to be rigidly attached to the target object. This marker body typically consists of a set of fiducials, which are either light-emitting or retro-reflective. During the process of tracking a target, the n-occular camera system generates 2D images of the fiducials . From the imaged 2D-marker position, the 3D position of the markers, the marker body and eventually of the tool can be determined. However, the accuracy of positioning is dependent on many factors. Among the predominant variables affecting this are the geometry of the system, light conditions, pose of the cameras and fiducial visibility. Using the approach proposed by Sielhorst et al. [10], the uncertainty is propagated using the internal camera parameter, camera poses, tracking body poses, body geometry and marker visibility, in order to estimate the expected accuracy . Thereby the tracking induced fiducial localization error (FLE) and the target registration error (TRE) are modeled as anisotropic non-uniform errors [9].

E. Intra-operative Visualization and Plan Update Based On 3D Freehand Ultrasound

Motivation. In order to validate the pre-operative plan intra-operatively and offer additional navigation and orientation for the surgeon, we incorporate 3D Freehand Ultrasound into the ROBOCAST system. In 3D Freehand Ultrasound, the probe of a conventional 2D ultrasound system is equipped with a dynamic reference frame (DRF) that is tracked by a 3D positioning system during the scan process, typically a manually performed sweep across the target anatomy. After a probe calibration step, the 2D ultrasound image is combined with its 3D pose information for each slice that is acquired. In a compounding step, an ultrasound volume is created. The usage of ultrasound intra-operatively helps the surgeon to carry over the pre-operative plan to the surgery room by offering a live update on the pre-operative imaging data and assess changes in anatomy due to effects such as brain shift [14]. In the results section, we present initial results demonstrating the visibility of macro-vasculature as well as surgical tooling such as a DBS electrode in transcranial ultrasound images. This indicates the possibility of offering intra-operative visual feedback on the probe trajectory executed by the robot.

Ultrasound Calibration. A crucial step in the acquisition of 3D Freehand Ultrasound consists in probe calibration. In this step, the spatial relation between the probe DRF and the ultrasound image is determined in form of a 4×4 calibration matrix ${}^{image}T_{DRF}$. After calibration, the coordinates of each pixel are known in 3D space. There are numerous methods for probe calibration and we refer the reader to [22] for a comprehensive review on various calibration methods and their strengths and weaknesses concerning precision, accuracy, phantom simplicity and usability for different probe types. Among the available methods for calibration, we chose to implement and integrate a Single Wall calibration into our system due to its satisfactory accuracy in combination with a high simplicity of the phantom. The average accuracy of this method is reported to be 2.46 mm with 0.39mm precision [22]. So far, we have implemented the calibration method and assessed the calibration outcome qualitatively through correct compounding of phantom objects. A detailed quantitative analysis of the calibration accuracy within the ROBOCAST project is current work in progress.

Ultrasound Freehand Volume Compounding. After successfully calibrating the ultrasound probe, we can combine ultrasound slices with the 3D pose of the transducer. The combination of both information for the forming of ultrasound volumes is performed in the compounding step. As a method, we have chosen Backward-Warping Ultrasound Reconstruction as proposed by Wein et al. [17]. Following their method, for every voxel x_i in the reconstruction volume V, we accumulate the intensities of all pixels p from neighboring ultrasound slices within a specified distance D and weight them according to their distance $d(x_i, p)$. We used Gaussian weighting in our experiments. Ultrasound MPR slices can be reconstructed from this volume rapidly and compared to optically co-registered slices from the patient's MRI volume.

IV. CURRENT PROGRESS AND PRELIMINARY RESULTS

A. First Results on Automatic Path Planning

We have studied the risk factors that are currently considered in keyhole neurosurgery path planning via interviews with several neurosurgeons in three hospitals in Germany, Italy and Israel. It was found that most of the risk factors can be represented in form of geometric constraints that can be computed and presented to the physician. For example the constraint "the nearest blood vessel should be at least 2mm

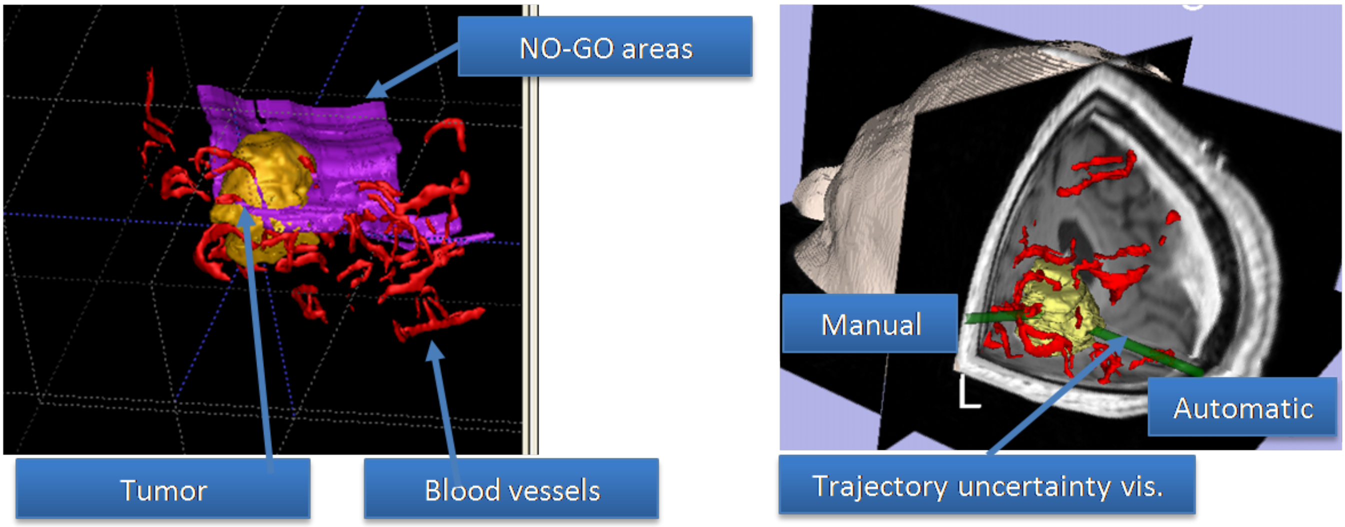

Fig. 1. Screenshot excerpts from our pre-operative planning modules. The left part image shows the definition of a target (tumor), geometric constraints for the trajectory in form of no-go areas and critical structures such as blood vessels combined into a crude risk atlas. The right image shows two automatically proposed trajectories with minimal risk (i.e. maximal distance to non-allowed regions). The incorporation of functional regions, fibres and statistical multi-patient anatomy into the risk atlas is currently under development.

from the path" can be computed, if a path (segment) and a segmentation of the blood vessels (volume) are given.

The path planning module was implemented and integrated into Slicer3. For this feasibility check, the user interface was not friendly enough for the neurosurgeon to use, so the authors have selected several 'safe' paths manually and without the path planning module guidance. Afterwards, we have computed the optimal path and compared the values of the geometrical parameters. Although we lack an assessment from a medical partner so far about the reasonability of the proposed trajectory, the computed optimal path was better than the manually selected paths, in the sense that a larger distance to the closest blood vessel or to the no-contraction zones could be achieved.

B. Localization Error Study

We retrospectively measure the localization error along the tool trajectory and on its tip for six consecutive patients who underwent keyhole minimally invasive Ommaya catheter placement surgery by three different neurosurgeons with a commercial neuronavigation system (Medtronic, USA). Firstly, the preoperative images (one MRI and five CTs with $0.47 \times 0.47 \times 1.0mm^3$ and $0.61 \times 0.61 \times 1.0mm^3$ resolutions) were fused with postoperative CT images showing the Ommaya catheter. Then, the localization errors were computed by comparing the preoperative planned surgical trajectory with the actual postoperative catheter position.

The mean TRE, ERE, ARE and SRE were $5.6mm(max = 12.0mm)$, $4.5mm(max = 5.8mm)$, $5.6^o(max = 16.0^o)$ and $2.6mm(max = 7.2mm)$, respectively. Note that low ARE and SRE do not necessary imply low TRE. For example, Patient 4 has ARE and SRE values that are much lower than those of Patient 1, but the observed TRE of Patient 4 was almost double than that of Patient 1. The TRE for Patient 1 was 3.7mm, which is clinically acceptable. However, 52mm before, at the cortical penetration point of the catheter, a significant catheter misplacement of 11.5mm was measured. At this location, the brain surface is rich with blood vessels, so a deviation of more than 10mm from the planned cortical penetration point may increase the risk of vascular injury. This shows that although the TRE is clinically acceptable, the localization error along the trajectory may not be acceptable. We continue to gather data and will incorporate it in the surgical path planning module.

C. First Results on Transcranial 3D Freehand Ultrasound Acquisition

Together with our medical partners, we were able to acquire transcranial ultrasound images on 3 participants, 2 of which were Parkinson patients who had recently undergone surgery for implantation of DBS electrodes. Transcranial ultrasound images were acquired through the temporal lobe where the skull bone is thin enough to allow ultrasound imaging at low frequencies of 2-3 MHz. On the first patient, we set up the equipment for 3D Freehand scanning and obtained several transcranial 3D ultrasound volumes at 2Mhz frequency and 14cm penetration depth in order to image the entire brain until the rear calotte of the skull. Additionally, we acquired Power Doppler and Color Doppler images. Colored pixels were filtered from the frame-grabbed ultrasound images in order to achieve a rough segmentation of blood vessels. Both the anatomy and the blood vessels were compounded separately. Through optical tracking, a registration of the volumes could be achieved. Two screenshots can be seen in figure 2. Throughout the progress of the project, we intend to overlay an MPR slice from the ultrasound volume with a spatially corresponding slice from the MR angiography volume, offering improved spatial context and an assessment of tissue shifts that occurred intra-operatively to the surgeon.

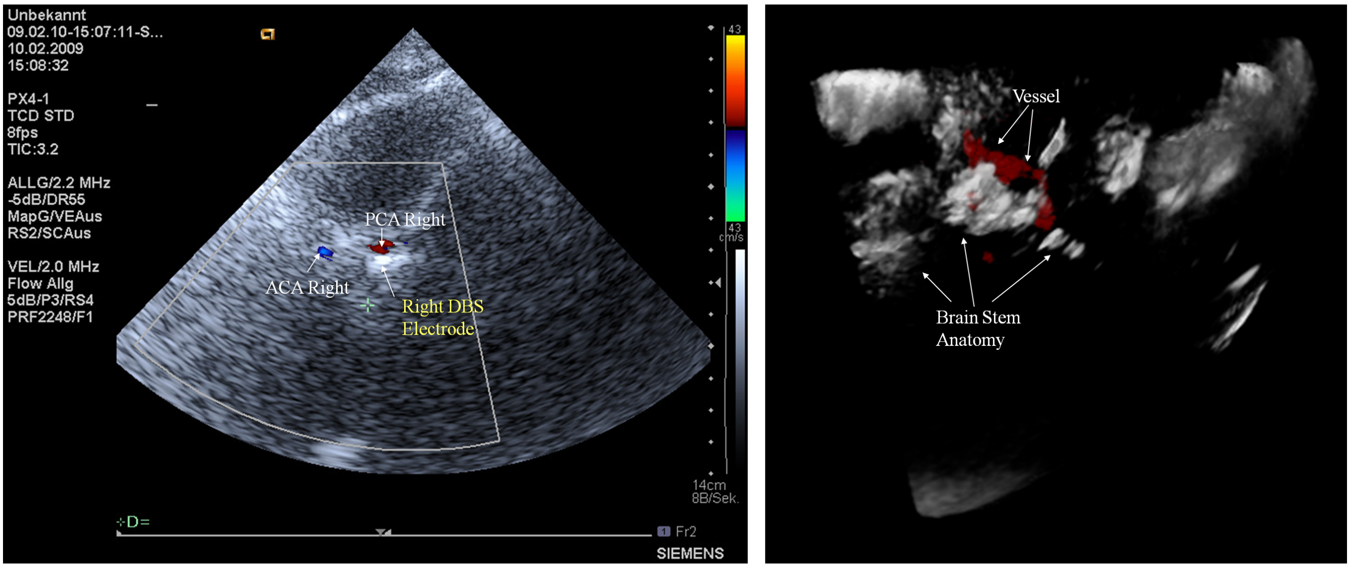

Fig. 2. Transcranial ultrasound scans of the basal ganglia in 2D on patient 1 (left) and in 3D on patient 2 (right). The cross-section of the DBS electrode in relation to the PCA (arteria cerebri posterior) can be clearly seen in patient 1. The right image shows a 3D reconstruction of the brain stem anatomy of patient 2 (white) and the reconstructed PCA vessel (red).

With the second patient, we conducted experiments on the visibility of a DBS electrode transcranially. In figure 2, a cross-section of the DBS electrode is displayed in spatial relation to a nearby vessel. We consider this as a breakthrough result for the ROBOCAST project, since this indicates the visibility of surgical tools in transcranial ultrasound images. Implicitly, this allows a safe and non-invasive localization of surgical tools inside the brain. In the upcoming year, we are going to investigate the accuracy of tool localization and navigation transcranially. Additionally, we investigate the accuracy and imaging quality of ultrasound imaging through the burr-hole as a second option. We expect the accuracy to be much higher due to direct contact with the dura and due to higher frequencies which increase image resolution, effectively increasing localization accuracy.

V. CONCLUSIONS AND FUTURE WORKS

Insertion of a surgical tool along a predefined trajectory with nearby sensitive structures such as blood vessels and eloquent areas is a common practice in keyhole neurosurgery. In some applications, e.g. Deep Brain Stimulation and Stereotactic Brain Biopsy, multiple targets along a single trajectory may be defined. Therefore, studying the localization errors along the planned trajectory is of clinical importance. Furthermore, the system uncertainty intra-operatively may lead to wrongly assumed security and to impaired decision making. Thus, it is calculated and visualized to the surgeon in an appropriate manner in the ROBOCAST system.

Our findings on the Ommaya catheter procedure provide a better understanding of accuracy in image guided surgery and aim at shifting the research focus from a single target error to the entire trajectory accuracy. We are currently developing a geometric uncertainty model that incorporates empirical clinical data and will assist the surgeon to preoperatively assess the surgical tool trajectory risk.

We presented the workflow of a comprehensive pre-operative planning wizard that incorporates several patient-specific medical images together with multi-patient statistical atlas data into a risk atlas. We presented methods for using a vessel-based risk map for automated proposition of paths with minimal risk. This vessel-based atlas will be augmented with further risk information in the upcoming year of the project. A simulation step at the end of the planning workflow ensures the compatibility of the probe with the spatial situation of robots and objects in the OR. At all times of surgical planning, the surgeon can decide to discard automatical trajectory suggestions and rely on traditional, manual methods for planning of the procedure.

We presented motivation and methods for the usage of 3D Freehand Ultrasound in neurosurgical keyhole surgery. First results indicate the value of transcranial ultrasound for visualization of macro-vasculature and surgical tooling such as DBS electrodes. Such information can help the surgeon to validate the trajectory that is being executed by the robot intra-operatively. In the next year, we are going to quantitatively evaluate the potential of this approach and also perform phantom experiments and cadaver experiments using burr-hole ultrasound.

In this paper, we have presented the combination of several existing and new methods for advanced planning of robotic neurosurgical procedures. The overall aim is to equip the ROBOCAST robotic system with software and validation tools for increased safety and comfort in planning and execution of complex minimally-invasive neurosurgical procedures with one or several targets.

VI. ACKNOWLEDGMENTS

We thank our medical partners from Italy (Dr. Kenneth Ricciardi, Prof. Massimo Gerosa, Neuroscience, Neuroradiological and Neurosurgery Departments, University of

Verona), from Israel (Dr. Yigal Shoshan and Dr. Zvi Israel, The Hadassah Ein-Karem University Hospital, Jerusalem) and from Germany (Dr. Jan Mehrkens and Dr. Kai Bötzel, Klinikum der LMU Großhadern, Munich). We also thank the entire ROBOCAST consortium for their collaboration and support.
This work was supported by EU grant FP7-ICT-2007-215190.

REFERENCES

[1] Ron Kikinis and Martha E. Shenton and Dan V. Iosifescu and Robert W. McCarley and Pairash Saiviroonporn and Hiroto H. Hokama and Andre Robatino and David Metcalf and Cynthia G. Wible and Chiara M. Portas and Robert M. Donnino and Ferenc A. Jolesz, A Digital Brain Atlas for Surgical Planning, Model Driven Segmentation and Teaching, *IEEE Transactions on Visualization and Computer Graphics*, vol. 2(3), 1996, pp 232-241

[2] Tom Vercauteren and Xavier Pennec and Aymeric Perchant and Nicholas Ayache, *Symmetric Log-Domain Diffeomorphic Registration: A Demons-based Approach*, Proceedings of the 11th International Conference on Medical Image Computing and Computer Assisted Intervention (MICCAI 2008), New York, NY, 1996

[3] Manniesing et al., Vessel enhancing diffusion – A scale space representation of vessel structures, *Medical Image Analysis*, vol. 10 (6), 2006, pp. 815-825

[4] A.F. Frangi and W.J. Niessen and K.L. Vincken and M.A. Viergever, Multiscale vessel enhancement filtering, Model Driven Segmentation and Teaching, *Medical Image Computing and Computer-Assisted Intervention (MICCAI)*, Lecture Notes in Computer Science, vol. 1496, vol. 2(3), 1996, pp 130-137

[5] A. Sboarina and R. Foroni and C. Lovato and A. De Simone and G. Fracastoro and A. Guglielmi and GK. Ricciardi and A. Nicolato and M. Longhi and F. Lupidi and M. Gerosa, Vascular visualization for surgery planning: skeletonization and tubular modeling, *Tenth Israeli Symposium on Computer-Aided Surgery (ISRACAS 2007)*, Medical Robotics, and Medical Imaging, Haifa, Israel, May 2007

[6] P. A. Yushkevich, J. Piven, C. Hazlett, H. Smith G. Smith, R. Ho, S. Ho, J. C. Gee and G. Gerig, User-Guided 3D Active Contour Segmentation of Anatomical Structures: Significantly Improved Efficiency and Reliability, *Neuroimage J.*, Vol. 31, 2006, pp 265-271.

[7] P. E. Danielson, Euclidean distance mapping, *Computer Vision, Graphics, and Image Processing*, Vol. 14, 1980, pp 227-248.

[8] L. Joskowicz, R. Shamir, M. Freiman, M. Shoham, E. Zehavi, F. Umansky and Y. Shoshan, Image-guided system with miniature robot for precise positioning and targeting in keyhole neurosurgery, *Computer Aided Surgery*, Vol. 11, 2006, pp 181-193.

[9] J. Michael Fitzpatrick and Jay B. West and Maurer, Jr., Calvin R., Predicting Error in Rigid-Body Point-Based Registration, *Transactions on Medical Imaging (TMI)*, Vol. 14, 1998, pp 694–702.

[10] T Sielhorst and M Bauer and O Wenisch and G Klinker, Online Estimation of the Target Registration Error for n-Ocular Optical Tracking Systems, *Medical Image Computing and Computer-Assisted Intervention (MICCAI)*, Lecture Notes in Computer Science, 2007

[11] Ellen J. L. Brunenberg and Anna Vilanova and Veerle Visser-Vandewalle and Yasin Temel and Linda Ackermans and Bram Platel and Bart M. ter Haar Romeny, Automatic Trajectory Planning for Deep Brain Stimulation: A Feasibility Study, *Medical Image Computing and Computer-Assisted Intervention (MICCAI)*, vol. 4791, 2007, pp. 584-592

[12] Yelnik, J. and Bardinet, E. and Dormon, D. and Malandain, G. and Ourselin, S. and Tande, D. and Karachi, C. and Ayache, N. and Cornu, P. and Agid, Y., A three-dimensional, histological and deformable atlas of the human basal ganglia. I. Atlas construction based on immunohistochemical and MRI data. *NeuroImage*, 34 (2), 2007, pp. 618-638

[13] Simpson, A. and Ma, B. and Chen, E. and Ellis, R. and Stewart, A., Using registration uncertainty visualization in a user study of a simple surgical task., *Medical Image Computing and Computer-Assisted Intervention (MICCAI)*, 2007

[14] I. A. Rasmussen and F. Lindseth and O. M. Rygh and E. M. Berntsen and T. Selbekk and J. Xu and T.A.N. Hernes and E. Harg and A. Hberg and G. Unsgaard, Functional neuronavigation combined with intra-operative 3D ultrasound: Initial experiences during surgical resections close to eloquent brain areas and future directions in automatic brain shift compensation of preoperative data, *Acta Neurochirurgia (Wien)*, vol. 149, 2007, pp 365-378

[15] Chakravarty MM and Sadikot AF and Mongia S and Bertrand G and Collins DL, Towards a multi-modal atlas for neurosurgical planning., *Med Image Comput Comput Assist Interv Int Conf Med Image Comput Comput Assist Interv.*, vol. 9(Pt 2), 2006, pp 389-96

[16] Pierre-Franois D'Haese and Ebru Cetinkaya and Peter E. Konrad and Chris Kao and Benoit M. Dawant, Computer-aided placement of deep brain stimulators: from planningto intraoperative guidance, *IEEE Trans. Med. Imaging*, vol. 24(11), 2005, pp. 1469-1478

[17] W. Wein and F. Pache and B. Roeper and N. Navab, Backward-Warping Ultrasound Reconstruction for Improving Diagnostic Value and Registration, *Medical Image Computing and Computer-Assisted Intervention (MICCAI)*, 2006

[18] Ting Guo and Andrew G. Parrent and Terry M. Peters, Automatic Target and Trajectory Identification for Deep Brain Stimulation (DBS) Procedures, *Medical Image Computing and Computer-Assisted Intervention (MICCAI)*, vol. 2791, 2007, pp. 483-490

[19] Marc Vaillant and Christos Davatzikos and Russell H. Taylor and R. Nick Bryan, A path-planning algorithm for image-guided neurosurgery, *Lecture Notes in Computer Science CVRMed-MRCAS'97*, vol. 1205, 1997, pp. 467-476

[20] N.M. Ivancevich and G.F. Pinton and S.W. Smith and H.A. Nicoletto and M. Scism and E. Bennett and D.T. Laskowitz, 7A-5 Real-Time 3D Contrast-Enhanced Transcranial Ultrasound, *Ultrasonics Symposium, 2007. IEEE*, vol. 1, 2007, pp. 550-553

[21] Pillai P and Sammet S and Ammirati M, Application accuracy of computed tomography-based, image-guided navigation of temporal bone, *Neurosurgery*, vol. 63(4 Suppl 2), 2008, pp. 326-33.

[22] Po-Wei Hsu and Richard W. Prager and Andrew H. Gee and Graham M. Treece, Freehand 3D Ultrasound Calibration: A Review , *Advanced Imaging in Biology and Medicine*, Springer Berlin Heidelberg, Vol. I, 2009, pp 47-84.

[23] Eljamel MS., Robotic Neurological Surgery Applications: Accuracy and Consistency or Pure Fantasy?, *Stereotact Funct Neurosurg*, Vol. 87, 2009, pp 88-93